

UC Berkeley

UC Berkeley Previously Published Works

Title

Vertebral fragility and structural redundancy.

Permalink

<https://escholarship.org/uc/item/6mc6f495>

Journal

Journal of bone and mineral research : the official journal of the American Society for Bone and Mineral Research, 27(10)

ISSN

0884-0431

Authors

Fields, Aaron J
Nawathe, Shashank
Eswaran, Senthil K
[et al.](#)

Publication Date

2012-10-01

DOI

10.1002/jbmr.1664

Peer reviewed



Published in final edited form as:

J Bone Miner Res. 2012 October ; 27(10): 2152–2158. doi:10.1002/jbmr.1664.

Vertebral fragility and structural redundancy

Aaron J. Fields¹, Shashank Nawathe¹, Senthil K. Eswaran¹, Michael G. Jekir¹, Mark F. Adams², Panayiotis Papadopoulos¹, and Tony M. Keaveny^{1,3}

¹Orthopaedic Biomechanics Laboratory, Department of Mechanical Engineering, University of California, Berkeley, CA, USA

²Department of Applied Physics and Applied Mathematics, Columbia University New York, NY, USA

³Department of Bioengineering, University of California, Berkeley, CA, USA

Abstract

The mechanisms of age-related vertebral fragility remain unclear, but may be related to the degree of “structural redundancy” of the vertebra, that is, its ability to safely redistribute stress internally after local trabecular failure from an isolated mechanical overload. To better understand this issue, we performed biomechanical testing and nonlinear micro-CT-based finite element analysis on 12 elderly human thoracic ninth vertebral bodies (ages 76.9 ± 10.8 years). After experimentally overloading the vertebrae to measure strength, we used the nonlinear finite element analysis to estimate the amount of failed tissue and understand failure mechanisms. We found that the amount of failed tissue per unit bone mass decreased with decreasing bone volume fraction ($r^2 = 0.66$, $p < 0.01$). Thus, for the weak vertebrae with low bone volume fraction, overall failure of the vertebra occurred after failure of just a tiny proportion of the bone tissue ($< 5\%$). This small proportion of failed tissue had two sources: the existence of fewer vertically oriented load paths to which load could be redistributed from failed trabeculae; and the vulnerability of the trabeculae in these few load paths to undergo bending-type failure mechanisms, which further weaken the bone. Taken together, these characteristics suggest that diminished structural redundancy may be an important aspect of age-related vertebral fragility: vertebrae with low bone volume fraction are highly susceptible to collapse since so few trabeculae are available for load redistribution if the external loads cause any trabeculae to fail.

Keywords

bone strength; finite element analysis; osteoporosis; vertebra; biomechanics

Corresponding author: Aaron J. Fields, Ph.D., 513 Parnassus Avenue, S-1161, University of California, San Francisco, CA 94143-0514, USA, (415) 476-0960, fax (415) 476-1128, fieldsa@orthosurg.ucsf.edu.

Please address all reprint requests to: Tony M. Keaveny, Ph.D., 6175 Etcheverry Hall, University of California, Berkeley, CA 94720-1740, USA, (510) 642-8017, fax (510) 642-6163, tmk@me.berkeley.edu

Disclosures:

Dr. Keaveny holds equity interests in O.N. Diagnostics. The other authors do not have any conflicts of interest.

Author Contributions

A.J.F. initiated the project, and with T.M.K., supervised the study. A.J.F., S.K.E., M.G.J. and T.M.K. conceived and designed the models and experiments. A.J.F. and S.N. performed the finite element simulations; A.J.F. and M.G.J. performed the experiments. M.F.A. and P.P. developed the parallel finite element framework. All authors analyzed the data and helped prepare the manuscript.

Introduction

Increased skeletal fragility is associated with aging and osteoporosis ⁽¹⁾ and is manifested by fragility fractures ⁽²⁾. While the precise meaning of ‘fragility’ is vague as far as fracture etiology is concerned, with many factors being involved ^(3,4), overall bone strength is an important aspect of fragility because it defines the biomechanical threshold at which point a fracture occurs ^(5,6). In this study, we investigated if the engineering concept of *structural redundancy* might provide insight into age-related changes in vertebral strength and fragility.

Structural redundancy is a key concept in structural engineering design ^(7,8), and refers to the ability of a structure to retain its function without catastrophic consequences — even when one or many parts of the structure fail. This is accomplished by providing multiple redundant load paths so that if one load path fails during normal operation or during an accident, stress can be redistributed internally from the failed parts to other parts of the structure and safe function is thus preserved. In such structurally redundant systems, overall failure of the structure requires failure of many parts. However, if structural redundancy is diminished, overall failure of the structure can occur if only a few parts fail. When a vertebra is loaded to overall failure, the amount of tissue that fails is unknown, and may depend on such factors as tissue material properties, bone volume fraction, cortical thickness, trabecular separation or a number of other measures of bone microarchitecture ^(9–14). Our prior work using isolated cores of trabecular bone has shown that the amount of tissue-level failure at the point of overall failure of the core decreases as bone volume fraction decreases ^(12,13). If the same were also true for the whole vertebra, this would suggest that vertebrae with low bone volume fraction are weak in part because of reduced structural redundancy.

To date, exploring structural redundancy in whole vertebrae has not been feasible owing to the technical challenge of performing the required biomechanical analysis. With the ability to perform fully nonlinear finite element analysis on high-resolution micro-CT images of whole vertebrae, we can now overcome this technical challenge. Thus, in the present study, we sought to quantify the amount of tissue failure that occurs at the onset of overall failure in elderly human vertebrae and in this manner elucidate mechanisms of bone fragility related to diminished structural redundancy.

Materials and Methods

Study design

Understanding the mechanisms of vertebral strength requires observing how load is transferred to individual trabeculae inside the vertebra while accounting for the deformation and failure mechanisms of those individual trabeculae. This is difficult to achieve through biomechanical testing alone ^(14,15), so we accomplished this by coupling biomechanical tests with high-resolution, micro-CT-based finite element analysis. The finite element simulations — experimentally validated in previous studies ^(11,16,17) — were calibrated here to a series of biomechanical tests in order to analyze the deformations inside the vertebra during an overload. This approach enabled us to relate vertebral strength at the whole-bone level to the failure mechanisms at the tissue-level. The failure mechanisms of the bone are greatly influenced by the bone’s microarchitecture. To account for variation in the failure mechanisms that arise because of variation in microarchitecture across the population, we analyzed multiple vertebrae exhibiting wide variation in trabecular bone volume fraction and architecture.

Specimen preparation and micro-CT scanning

Twelve whole thoracic ninth (T9) vertebrae were obtained fresh frozen from human cadaver spines (age 76.9 ± 10.8 years, range 53–97 years) with no history of metabolic bone disorders. We chose to study the T9 vertebra because of its high fracture incidence⁽¹⁸⁾ and, because of its smaller size relative to the more frequently fractured L1 vertebra, analysis of the T9 vertebrae made for slightly smaller finite element models. As described previously in more detail⁽¹⁹⁾, the posterior elements were removed and each isolated vertebral body was micro-CT imaged with a 30- μm voxel size (Scanco 80; Scanco Medical AG; Brüttisellen, Switzerland). The images were coarsened to a 60- μm voxel size, and the hard tissue and marrow were segmented using a global threshold value. Standard microarchitecture measures were calculated using the coarsened images: trabecular bone volume fraction; mean trabecular thickness (Tb.Th*); mean trabecular separation (Tb.Sp*); mean trabecular number (Tb.N*); structural model index (SMI); and degree of anisotropy (DA).

Biomechanical testing

After micro-CT imaging, we performed experimental compression tests to measure vertebral strength, using an established testing protocol^(19–21). Briefly, the vertebral bodies were first placed between polymethyl methacrylate (PMMA) endcaps to ensure plano-parallel ends^(22,23). Next, the top platen of a screw-driven load frame was lowered onto the vertebra; a lockable ball joint ensured the top platen rested flat on the vertebra during loading. Compression was performed in displacement control at a slow strain rate ($\sim 0.05\text{--}0.5\%$ strain/s) after cyclic preconditioning⁽¹⁹⁾. Vertebral strength was defined as the peak force achieved during the loading cycle.

Finite element analysis

To study the failure mechanisms of the vertebrae, we performed fully nonlinear finite element analysis of the micro-CT scans. High-resolution finite element models of the vertebrae were created from the coarsened micro-CT images by converting each cubic voxel in the images into an eight-noded, 60- μm brick element^(24,25). A numerical convergence study (Appendix 1) indicated that models with this element size accurately captured the inter-specimen variation in failure mechanisms compared to models with a 30- μm element size (Figure A1). Geometrically and materially nonlinear finite element analysis^(11,26) was conducted for each model to 1% apparent compressive strain. The models were virtually compressed via simulated layers of PMMA (elastic modulus 2.5 GPa and Poisson's ratio of 0.3) to mimic the boundary conditions used in the biomechanical tests. Bone tissue was modeled using a rate-independent elasto-plasticity model⁽²⁷⁾ and homogeneous isotropic⁽²⁸⁾ tissue material properties: elastic modulus 5 GPa, Poisson's ratio of 0.3, and tissue-level tensile and compressive yield strains of 0.33% and 0.81%, respectively⁽¹¹⁾.

In terms of numbers of degrees of freedom and CPU requirements, the overall size of this computational analysis represents one of the largest published numerical structural analysis problems. Individual models contained up to 485 million elements (over 1.5 billion degrees of freedom) and were solved using an implicit, parallel finite element framework⁽²⁹⁾. The nonlinear solution algorithm was an inexact Newton method wherein each Newton iteration was solved using an algebraic multigrid solver. All simulations were performed on the Sun Constellation Cluster at the Texas Advanced Computing Center, requiring an equivalent single-processor time of 72 years (a typical analysis required 15 hours of real time using 2000 processors in parallel).

Several outcomes from the finite element analyses were used to characterize the failure mechanisms. Vertebral strength was determined from the force-strain curve using the 0.2% offset method. Comparison of model-predicted vertebral strength to measured strength for

these vertebrae (Appendix 2) indicated that the models had statistical $Y = X$ type accuracy ($r^2 = 0.85$, Figure A2). The number and loading mode of failed Gauss points in the models was assessed at each step of the analysis to quantify the location and amount of failed tissue. We evaluated tissue failure at the Gauss points since previous work on trabecular bone cores found that this approach substantially reduces the error in quantifying the proportion of failed tissue compared to evaluating failed tissue at element corners⁽³⁰⁾. The proportion of failed tissue was calculated as the number of failed Gauss points at the vertebra's overall yield strength divided by the total number of Gauss points in the model (excluding the PMMA). This outcome represents the amount of failed tissue per unit bone mass.

Statistics

The total proportion of failed tissue, as well as the proportions of failed tissue in compression and in tension, was related to vertebral strength using univariate regression. Multivariate (stepwise) regression was used to adjust for the effect of bone volume fraction on vertebral strength. All statistical tests (JMP 7.0; SAS Institute, Cary, NC USA) were taken as significant at $p < 0.05$.

Results

The proportion of failed tissue in the vertebrae with the lowest BV/TV represented only a tiny amount (< 5%) of the overall bone tissue (Figures 1 & 2A). For the low-BV/TV vertebrae, the failed tissue was highly localized to just a few load paths consisting of parallel columns of vertically oriented trabecular bone. In contrast, for the high-BV/TV vertebrae, the failed tissue was widespread, being distributed over numerous load paths that consisted of both the trabecular bone and the cortical shell (Figure 1). As expected, the low-BV/TV vertebrae were also weaker than the high-BV/TV vertebrae ($r = -0.75$, $p = 0.005$, $n = 12$ vertebrae). In addition to being weaker because they had less bone tissue, the weak vertebrae had significantly less failed tissue than the strong vertebrae ($p = 0.01$ after adjusting for the effect of BV/TV).

Another difference between the low- and high-BV/TV vertebrae was a shift in the failure mechanisms of the tissue. The fivefold variation in the total amount of failed tissue across vertebrae primarily reflected a large difference in the amount of tissue exceeding the compressive yield strain (Figure 2A). This difference betrays a shift in the failure mechanisms: a greater amount of tissue exceeding the compressive yield strain indicates that axial compression of individual trabeculae dominates the deformation mechanism, whereas an equal amount of tissue exceeding the compressive and tensile yield strains indicates that bending of individual trabeculae dominates. In the vertebrae with high bone volume fraction, up to four times more tissue failed in compression than in tension (Figure 2B,C). In the vertebrae with the lowest bone volume fraction, however, nearly equal amounts of tissue failed in compression and in tension, and the failed tissue was localized to opposite sides of slender, rod-like trabeculae that underwent excessive bending (Figure 2D). Animations of the deforming microstructure for vertebrae with decreasing bone volume fraction further illustrate the shift toward bending-type deformations (see animations accompanying the online version of this article).

We found several noteworthy relationships between the proportion of failed tissue and parameters describing the average characteristics of the trabecular microarchitecture. The proportion of failed tissue was significantly lower in vertebrae that had fewer trabeculae (Tb.N: $r = 0.61$, $p = 0.03$). However, given that the number of trabeculae is correlated with bone volume fraction, it is difficult to separate these effects. One characteristic that is largely independent of bone volume fraction is the proportion of trabeculae that are

vertically aligned⁽³¹⁾. Vertebrae with a lower proportion of vertically aligned trabeculae had significantly less failed tissue (vBV/BV : $r = 0.64$, $p = 0.02$).

Discussion

These results reveal that vertebrae with low bone volume fraction are susceptible to overall vertebral failure after failure of just a tiny proportion of the bone tissue — this indicates that they lack structural redundancy, a hallmark of fragility. The small proportion of failed tissue in these weak vertebrae reflected two factors that occur for low-BV/TV vertebrae: the existence of fewer vertically oriented load paths to which load could be redistributed, and the tendency for these load paths to undergo bending-type deformations that preclude appreciable tissue failure. Moreover, we found that weak vertebrae had significantly less failed tissue than strong vertebrae, even after adjusting for the effect of either bone mass or volume fraction. This suggests that the amount of failed tissue at the point of overall vertebral failure may represent an insightful phenotype of bone quality^(32,33). Structural engineers design important load-bearing structures, *e.g.* buildings and bridges, with multiple redundant load paths so that when one load path fails, the structure can retain its function without catastrophic consequences, facilitating the repair of the damaged part. While vertebrae with high bone volume fraction appear to operate in a similar manner, in vertebrae with low bone volume fraction this structural redundancy is substantially diminished. Taken together, these findings provide new insight into the mechanisms of reduced vertebral fragility: not only are low-BV/TV vertebrae weaker than high-BV/TV vertebrae because they have less bone tissue, but they are also less structurally redundant — that is, they are susceptible to collapse from failure of just a tiny amount of bone tissue.

The concept of structural redundancy as applied to vertebral fragility is novel, and may provide new insight into the mechanisms of osteoporotic vertebral fractures. Although structural redundancy is a key aspect that governs the fragility of engineering structural systems^(7,8), we are not aware of any reports applying the concept of structural redundancy to the etiology of osteoporotic fractures. For example, a number of studies assessed the mechanical consequences of tissue damage or failure^(34–37), but none quantified the amount of failure required before overall failure of the bone. Our key finding is that overall failure of the elderly low-BV/TV vertebra occurs after failure of just a few load paths. This finding provides the first evidence that increased vertebral fragility with aging and osteoporosis may reflect a loss in both strength and structural redundancy. While thinning of horizontal trabeculae and resorption of vertical trabeculae⁽³⁸⁾ has been previously shown to compromise trabecular bone strength by making the microstructure more susceptible to bending and buckling^(34,36,39,40), it is possible for the microstructure to undergo bending and yet still have many redundant load paths. Rather, the weakest vertebrae exhibited bending-type deformations *and* a loss in structural redundancy. It is widely understood that bone fragility results from three factors⁽⁴⁾: 1) decreased bone mass; 2) deteriorated microstructure; and 3) diminished tissue material properties. Hence, our findings suggest a fourth factor in the pathogenesis of bone fragility, at least for the elderly vertebra: decreased structural redundancy. In a sense, decreased structural redundancy is the biomechanical mechanism by which deteriorated microstructure can influence bone strength independent of bone mass.

The finding that tissue failure can occur well before overall structural collapse is consistent with previous studies^(41,42) and provides insight into the different effects that accumulating failed tissue may have on the progression of vertebral deformities in low- versus high-BV/TV bone. The vertebrae with low BV/TV had few alternative load paths, and hence, local failure of just a few of the primary load paths in such vertebrae may accelerate the progression of a vertebral deformity upon reloading. This same mechanism may explain

why the reduction in vertebral strength following an isolated overload is greater in vertebrae with lower BV/TV and fewer trabeculae^(20,43). However, given the challenge relating finite element predictions of failed tissue with direct observations of microdamage^(44,45), additional research is required to understand the mechanism by which microdamage accumulation reduces bone strength⁽⁴⁶⁾. Our results indicate that such research may provide new insight into the interactions among bone volume fraction and architecture, the accumulation of failed tissue, changes in tissue-level ductility, and the failure mechanisms of the vertebra. For example, tissue ductility is known to decrease with increased age for cortical tissue^(47,48), and if the same is true for trabecular tissue, it is reasonable to hypothesize that decreases in tissue ductility might accentuate the biomechanical consequences of diminished structural redundancy.

A unique feature of this study design was our combined experimental and computational approach. Elucidating the role of diminished structural redundancy would have been challenging using experiments alone, since assessing structural redundancy requires quantifying the amount of failed tissue and understanding how load is transferred among individual trabeculae. In the absence of any experimental analysis techniques for such purposes, fully nonlinear micro-CT-based finite element analysis — although computationally very expensive — is perhaps the only feasible recourse. Indeed, a major technical innovation of this study was our ability to perform such a complex and large computational problem^(29,49). As high-fidelity analyses of this type become more widespread^(25,50), it should be possible to apply this technique to larger cohorts to gain a more complete understanding of age-related bone fragility.

Our analysis has a number of limitations. In generalizing our findings to other thoracic levels and to the lumbar spine, we note that our study did not account for any potential differences in overall kinematics and loading, the contribution of the posterior elements, or the presence of the ribs, but instead focused on the behavior of the isolated vertebral body. For the isolated vertebral body, the main factors are whether the bone is sufficiently large and the mechanics of internal load transfer are similar. To that end, we observe the following: 1) lumbar vertebrae are larger than thoracic vertebrae; 2) isolated samples of trabecular bone from the lumbar vertebra undergo a shift in failure mechanisms with decreasing BV/TV⁽¹¹⁾; 3) the number of vertical trabeculae in the lumbar spine decreases as BV/TV decreases^(38,51); and 4) cortical-trabecular load-sharing characteristics are similar between lumbar⁽²⁵⁾ and lower thoracic⁽²⁴⁾ vertebrae. These data suggest that diminished structural redundancy may help explain the increased fragility of the elderly lumbar vertebra too. As the vertebrae become much smaller though, it is unclear how the present findings apply since the mechanics of internal load transfer may differ, as may the overall BV/TV and the cortical-to-trabecular ratio. Likewise, it is unclear how these findings apply to other anatomic sites like the distal radius^(52,53) or proximal femur⁽⁵⁴⁾, since the amount of failed tissue at these sites may also depend on the mechanics of load transfer and overall boundary conditions.

It is appreciated that our assessment of the failure mechanisms remains purely computational at this point — that is to say, we have not directly measured the amount or location of failed tissue. The models themselves were well-validated against direct measures of whole-bone strength for these vertebrae (Appendix 2) and the predicted failure mechanisms agree qualitatively with experimental observations reported for isolated specimens of trabecular bone^(14,17). However, the precise nature of the nonlinear constitutive model for bone tissue is not known and thus represents a source of uncertainty and a topic for future research. Our assumed constitutive model was plasticity-based⁽¹⁶⁾ and used a failure criterion in principal strains that, according to known behavior of cortical bone, gave the tissue higher strength in compression than in tension⁽⁵⁵⁾. That constitutive

model did not simulate trabecular fracture since individual trabeculae rarely fracture before the apparent yield point^(42,56,57) and since we included large deformation effects in the models to account for the increased compliance of any individual trabeculae that had become excessively loaded⁽¹¹⁾. The models also did not account for any failure of the endplate tissue. Endplate failure is expected to add to the amount of failed tissue, although the behavior of the endplates, including any influence of the intervertebral disc^(58,59), is poorly understood. It is within this context that we view the absolute predictions of the models with caution. Nevertheless, our interpretation regarding the lower amount of failed tissue in vertebrae with lower BV/TV remains valid since the underlying mechanisms — the reduced number of load paths and the transition from axial deformation to bending — should be robust to these limitations. Indeed, the underlying mechanisms appear to be more sensitive to the overall trabecular and cortical architecture, which dictates how loads are transferred through the vertebra and distributed among individual trabeculae, than to the local geometric features and assumed material properties of any individual trabeculae (see Appendices 1 and 3).

In summary, these findings showed that in addition to being weak, vertebrae with low bone volume fraction were less structurally redundant because overall vertebral failure was associated with just a tiny amount of local tissue failure. This diminished structural redundancy in vertebrae with low bone volume fraction was the result of a small number of vertically oriented load paths and the predominance of bending-type failure mechanisms. These results suggest that diminished structural redundancy may be an important etiologic aspect of age-related vertebral fragility.

Supplementary Material

Refer to Web version on PubMed Central for supplementary material.

Acknowledgments

Funding for this study was provided by the National Institutes of Health (grants AR049828 and AR043784). Computational resources were made available through the National Science Foundation via TeraGrid (grant TG-MCA00N019). Human tissue was obtained from National Disease Research Interchange, UCSF, and Southeast Tissue Alliance. We thank Dr. Michael Liebschner (Baylor College of Medicine) for micro-CT imaging the vertebral bodies. T.M.K. has a financial interest in O.N. Diagnostics, and both he and the company may benefit from the results of this research.

References

1. Sambrook P, Cooper C. Osteoporosis. *Lancet*. 2006; 367(9527):2010–8. [PubMed: 16782492]
2. Elliot-Gibson V, Bogoch ER, Jamal SA, Beaton DE. Practice patterns in the diagnosis and treatment of osteoporosis after a fragility fracture: a systematic review. *Osteoporos Int*. 2004; 15(10):767–78. [PubMed: 15258724]
3. Seeman E. Pathogenesis of bone fragility in women and men. *Lancet*. 2002; 359(9320):1841–50. [PubMed: 12044392]
4. Turner CH. Biomechanics of bone: determinants of skeletal fragility and bone quality. *Osteoporos Int*. 2002; 13(2):97–104. [PubMed: 11905527]
5. Keaveny TM, Bouxsein ML. Theoretical implications of the biomechanical fracture threshold. *J Bone Miner Res*. 2008; 23(10):1541–7. [PubMed: 18410232]
6. Melton LJ 3rd, Riggs BL, Keaveny TM, Achenbach SJ, Hoffmann PF, Camp JJ, Rouleau PA, Bouxsein ML, Amin S, Atkinson EJ, Robb RA, Khosla S. Structural determinants of vertebral fracture risk. *J Bone Miner Res*. 2007; 22(12):1885–92. [PubMed: 17680721]
7. Feng YS, Moses F. Optimum Design, Redundancy and Reliability of Structural Systems. *Computers & Structures*. 1986; 24(2):239–251.

8. Schafer BW, Bajpai P. Stability degradation and redundancy in damaged structures. *Engineering Structures*. 2005; 27(11):1642–1651.
9. Gibson LJ. The mechanical behavior of cancellous bone. *J Biomech*. 1985; 18(5):317–328. [PubMed: 4008502]
10. Keaveny TM. Mechanistic approaches to analysis of trabecular bone. *Forma*. 1997; 12:267–275.
11. Bevill G, Eswaran SK, Gupta A, Papadopoulos P, Keaveny TM. Influence of bone volume fraction and architecture on computed large-deformation failure mechanisms in human trabecular bone. *Bone*. 2006; 39(6):1218–25. [PubMed: 16904959]
12. Bevill G, Farhamand F, Keaveny TM. Heterogeneity of yield strain in low-density versus high-density human trabecular bone. *J Biomech*. 2009; 42(13):2165–70. [PubMed: 19700162]
13. Morgan EF, Bayraktar HH, Yeh OC, Majumdar S, Burghardt A, Keaveny TM. Contribution of inter-site variations in architecture to trabecular bone apparent yield strains. *J Biomech*. 2004; 37(9):1413–20. [PubMed: 15275849]
14. Nazarian A, Müller R. Time-lapsed microstructural imaging of bone failure behavior. *J Biomech*. 2004; 37(1):55–65. [PubMed: 14672568]
15. Bay BK, Yerby SA, McLain RF, Toh E. Measurement of strain distributions within vertebral body sections by texture correlation. *Spine*. 1999; 24(1):10–17. [PubMed: 9921585]
16. Niebur GL, Feldstein MJ, Yuen JC, Chen TJ, Keaveny TM. High-resolution finite element models with tissue strength asymmetry accurately predict failure of trabecular bone. *J Biomech*. 2000; 33:1575–1583. [PubMed: 11006381]
17. Verhulp E, Van Rietbergen B, Müller R, Huiskes R. Micro-finite element simulation of trabecular-bone post-yield behaviour--effects of material model, element size and type. *Comput Methods Biomech Biomed Engin*. 2008; 11(4):389–95. [PubMed: 18568833]
18. Cooper C, Atkinson EJ, O’Fallon WM, Melton LJ. Incidence of clinically diagnosed vertebral fractures: a population-based study in Rochester, Minnesota, 1985–1989. *J Bone Miner Res*. 1992; 7:221–227. [PubMed: 1570766]
19. Fields AJ, Eswaran SK, Jekir MG, Keaveny TM. Role of trabecular microarchitecture in whole-vertebral body biomechanical behavior. *J Bone Miner Res*. 2009; 29(9):1523–30. [PubMed: 19338454]
20. Kopperdahl DL, Pearlman JL, Keaveny TM. Biomechanical consequences of an isolated overload on the human vertebral body. *J Orthop Res*. 2000; 18:685–690. [PubMed: 11117287]
21. Buckley JM, Loo K, Motherway J. Comparison of quantitative computed tomography-based measures in predicting vertebral compressive strength. *Bone*. 2007; 40 (3):767–74. [PubMed: 17174619]
22. Eriksson SAV, Isberg BO, Lindgren JU. Prediction of vertebral strength by dual photon-absorptiometry and quantitative computed-tomography. *Calcif Tissue Int*. 1989; 44 (4):243–250. [PubMed: 2501006]
23. Faulkner KG, Cann CE, Hasegawa BH. Effect of bone distribution on vertebral strength: assessment with patient-specific nonlinear finite element analysis. *Radiology*. 1991; 179(3):669–74. [PubMed: 2027972]
24. Eswaran SK, Gupta A, Adams MF, Keaveny TM. Cortical and trabecular load sharing in the human vertebral body. *J Bone Miner Res*. 2006; 21(2):307–14. [PubMed: 16418787]
25. Homminga J, Van-Rietbergen B, Lochmüller EM, Weinans H, Eckstein F, Huiskes R. The osteoporotic vertebral structure is well adapted to the loads of daily life, but not to infrequent “error” loads. *Bone*. 2004; 34(3):510–6. [PubMed: 15003798]
26. Stölken JS, Kinney JH. On the importance of geometric nonlinearity in finite-element simulations of trabecular bone failure. *Bone*. 2003; 33(4):494–504. [PubMed: 14555252]
27. Papadopoulos P, Lu J. A general framework for the numerical solution of problems in finite elastoplasticity. *Comput Methods Appl Mech Eng*. 1998; 159(1–2):1–18.
28. Kabel J, van Rietbergen B, Dalstra M, Odgaard A, Huiskes R. The role of an effective isotropic tissue modulus in the elastic properties of cancellous bone. *J Biomech*. 1999; 32(7):673–80. [PubMed: 10400354]

29. Adams, MF.; Bayraktar, HH.; Keaveny, TM.; Papadopoulos, P. Ultrascale implicit finite element analyses in solid mechanics with over a half a billion degrees of freedom. *ACM/IEEE Proceedings of SC2004: High Performance Networking and Computing*; 2004.
30. Niebur GL, Yuen JC, Hsia AC, Keaveny TM. Convergence behavior of high-resolution finite element models of trabecular bone. *J Biomech Eng.* 1999; 121(6):629–635. [PubMed: 10633264]
31. Fields AJ, Lee GL, Liu XS, Jekir MG, Guo XE, Keaveny TM. Influence of vertical trabeculae on the compressive strength of the human vertebra. *J Bone Miner Res.* 2011; 26(2):263–9. [PubMed: 20715186]
32. Heaney RP. Is the paradigm shifting? *Bone.* 2003; 33(4):457–65. [PubMed: 14555248]
33. Hernandez CJ, Keaveny TM. A biomechanical perspective on bone quality. *Bone.* 2006; 39(6): 1173–81. [PubMed: 16876493]
34. Guo XE, Kim CH. Mechanical consequence of trabecular bone loss and its treatment: a three-dimensional model simulation. *Bone.* 2002; 30(2):404–11. [PubMed: 11856649]
35. Kopperdahl DL, Roberts AD, Keaveny TM. Localized damage in vertebral bone is most detrimental in regions of high strain energy density. *J Biomech Eng.* 1999; 121:622–28. [PubMed: 10633263]
36. Silva MJ, Gibson LJ. Modeling the mechanical behavior of vertebral trabecular bone: Effects of age-related changes in microstructure. *Bone.* 1997; 21(2):191–199. [PubMed: 9267695]
37. Yeh OC, Keaveny TM. The relative roles of microdamage and microfracture in the mechanical behavior of trabecular bone. *J Orthop Res.* 2001; 19:1001–1007. [PubMed: 11780997]
38. Thomsen JS, Ebbesen EN, Mosekilde L. Age-related differences between thinning of horizontal and vertical trabeculae in human lumbar bone as assessed by a new computerized method. *Bone.* 2002; 31(1):136–142. [PubMed: 12110426]
39. Nazarian A, Stauber M, Zurakowski D, Snyder BD, Muller R. The interaction of microstructure and volume fraction in predicting failure in cancellous bone. *Bone.* 2006; 39 (6):1196–202. [PubMed: 16920051]
40. Snyder BD, Piazza S, Edwards WT, Hayes WC. Role of trabecular morphology in the etiology of age-related vertebral fractures. *Calcif Tissue Int.* 1993; 53S(1):S14–S22. [PubMed: 8275369]
41. Liu XS, Bevill G, Keaveny TM, Sajda P, Guo XE. Micromechanical analyses of vertebral trabecular bone based on individual trabeculae segmentation of plates and rods. *J Biomech.* 2009; 42(3):249–56. [PubMed: 19101672]
42. Nagaraja S, Couse TL, Guldberg RE. Trabecular bone microdamage and microstructural stresses under uniaxial compression. *J Biomech.* 2005; 38(4):707–16. [PubMed: 15713291]
43. Wegrzyn J, Roux JP, Arlot ME, Boutroy S, Vilayphiou N, Guyen O, Delmas PD, Chapurlat R, Bouxsein ML. Determinants of the mechanical behavior of human lumbar vertebrae after simulated mild fracture. *J Bone Miner Res.* 2011; 26(4):739–46. [PubMed: 20928886]
44. Green JO, Nagaraja S, Diab T, Vidakovic B, Guldberg RE. Age-related changes in human trabecular bone: Relationship between microstructural stress and strain and damage morphology. *J Biomech.* 2011; 44(12):2279–85. [PubMed: 21724189]
45. Shi X, Liu XS, Wang X, Guo XE, Niebur GL. Effects of trabecular type and orientation on microdamage susceptibility in trabecular bone. *Bone.* 2010; 46(5):1260–6. [PubMed: 20149908]
46. Burr DB, Forwood MR, Fyhrie DP, Martin RB, Schaffler MB, Turner CH. Bone microdamage and skeletal fragility in osteoporotic and stress fractures. *J Bone Miner Res.* 1997; 12(1):6–15. [PubMed: 9240720]
47. Burstein AH, Reilly DT, Martens M. Aging of bone tissue: mechanical properties. *J Bone Joint Surg Am.* 1976; 58(1):82–6. [PubMed: 1249116]
48. McCalden RW, McGeough JA, Barker MB, Court-Brown CM. Age-related changes in the tensile properties of cortical bone. The relative importance of changes in porosity, mineralization, and microstructure. *J Bone Joint Surg Am.* 1993; 75 (8):1193–205. [PubMed: 8354678]
49. Arbenz P, van Lenthe GH, Mennel U, Müller R, Sala M. A scalable multi-level preconditioner for matrix-free μ -finite element analysis of human bone structures. *Int J Num Meth Engg.* 2008; 73:927–47.

50. Verhulp E, van Rietbergen B, Muller R, Huiskes R. Indirect determination of trabecular bone effective tissue failure properties using micro-finite element simulations. *J Biomech.* 2008; 41(7): 1479–85. [PubMed: 18423473]
51. Liu S, Sajda P, Saha PK, Wehrli FW, Bevil G, Keaveny TM, Guo XE. Complete volumetric decomposition of individual trabecular plates and rods and its morphological correlations with anisotropic elastic moduli in human trabecular bone. *J Bone Miner Res.* 2008; 23(2):223–35. [PubMed: 17907921]
52. Pistoia W, van Rietbergen B, Lochmuller EM, Lill CA, Eckstein F, Ruegsegger P. Estimation of distal radius failure load with micro-finite element analysis models based on three-dimensional peripheral quantitative computed tomography images. *Bone.* 2002; 30(6):842–8. [PubMed: 12052451]
53. Vilayphiou N, Boutroy S, Szulc P, van Rietbergen B, Munoz F, Delmas PD, Chapurlat R. Finite element analysis performed on radius and tibia HR-pQCT images and fragility fractures at all sites in men. *J Bone Miner Res.* 2011; 26(5):965–73. [PubMed: 21541999]
54. Verhulp E, van Rietbergen B, Huiskes R. Load distribution in the healthy and osteoporotic human proximal femur during a fall to the side. *Bone.* 2008; 42(1):30–5. [PubMed: 17977813]
55. Reilly DT, Burstein AH. The elastic and ultimate properties of compact bone tissue. *J Biomech.* 1975; 8:393–405. [PubMed: 1206042]
56. Fyhrie DP, Schaffler MB. Failure mechanisms in human vertebral cancellous bone. *Bone.* 1994; 15(1):105–9. [PubMed: 8024844]
57. Wachtel EF, Keaveny TM. Dependence of trabecular damage on mechanical strain. *J Orthop Res.* 1997; 15:781–787. [PubMed: 9420610]
58. Fields AJ, Lee GL, Keaveny TM. Mechanisms of initial endplate failure in the human vertebral body. *J Biomech.* 2010; 43:3126–31. [PubMed: 20817162]
59. Pollintine P, Dolan P, Tobias JH, Adams MA. Intervertebral disc degeneration can lead to “stress-shielding” of the anterior vertebral body: a cause of osteoporotic vertebral fracture? *Spine.* 2004; 29(7):774–82. [PubMed: 15087801]
60. Crawford RP, Cann CE, Keaveny TM. Finite element models predict in vitro vertebral body compressive strength better than quantitative computed tomography. *Bone.* 2003; 33(4):744–50. [PubMed: 14555280]

Appendix 1

A numerical convergence study was performed to determine the effect of element size on the proportion of failed tissue — the main outcome from the analyses. We analyzed five models using a 30- μm element size and examined the relationship between the proportion of failed tissue and bone volume fraction. Results indicated that using 60 μm -sized elements overestimates the proportion of failed tissue compared to the finer model ($p < 0.05$, paired t-test), but the effect is small, particularly when compared to the difference in the proportion of failed tissue between vertebrae. Importantly, the overall trend is the same: there is less failed tissue per unit bone mass in vertebrae with lower bone volume fraction (Figure A1). Thus, using the models with the larger element size should not alter our conclusions.

Appendix 2

To support model validity, we compared predictions of whole-vertebral strength from the finite element models against direct measurements of vertebral strength from experiments. Results indicated a strong correlation between experiment and model, with statistical $Y = X$ type of agreement (Figure A2). Additionally, the nonlinear finite element modeling technique that we used for these whole-bone models has been well validated for trabecular bone cores — *e.g.* load-displacement curve-fits between experiment and model with $r^2 = 0.79\text{--}0.97$ ⁽⁵⁰⁾ — where experimental boundary conditions can be replicated numerically.

Appendix 3

A material sensitivity study was performed to determine the effect of changes to the assumed tissue material properties on the proportion of failed tissue. We reduced the assumed value of the compressive yield strength of the bone tissue by 15% in vertebrae with low and high bone volume fractions. This reduction in tissue compressive strength increased the proportion of failed tissue from 3.2% to 3.9% in the low-BV/TV vertebra, and from 13.7% to 17.3% in the high-BV/TV vertebra. Thus, while the proportion of failed tissue in any one vertebra was sensitive to the assumed material properties, the size of the effect across vertebrae was small when compared to the overall effect of inter-bone variations in bone volume fraction and architecture and whole-bone size and shape.

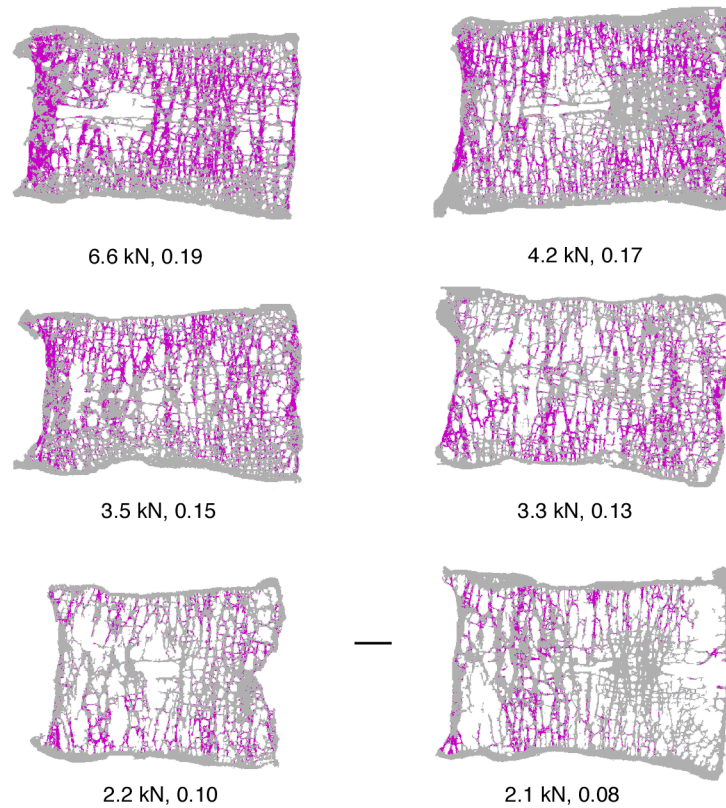


Figure 1. Mid-sagittal sections from human thoracic vertebrae showing the distribution of failed tissue (purple) at each vertebra's compressive strength. During an overload, the weak vertebrae with low bone volume fraction sustained relatively less failed tissue than the strong vertebrae with high bone volume fraction indicating that the former are less structurally robust. Vertebral strength, bone volume fraction given; scale bar, 5 mm; section thickness, 1 mm; left side, anterior. (The reader is also referred to animations of the deforming microstructure; please see the online version of this article.)

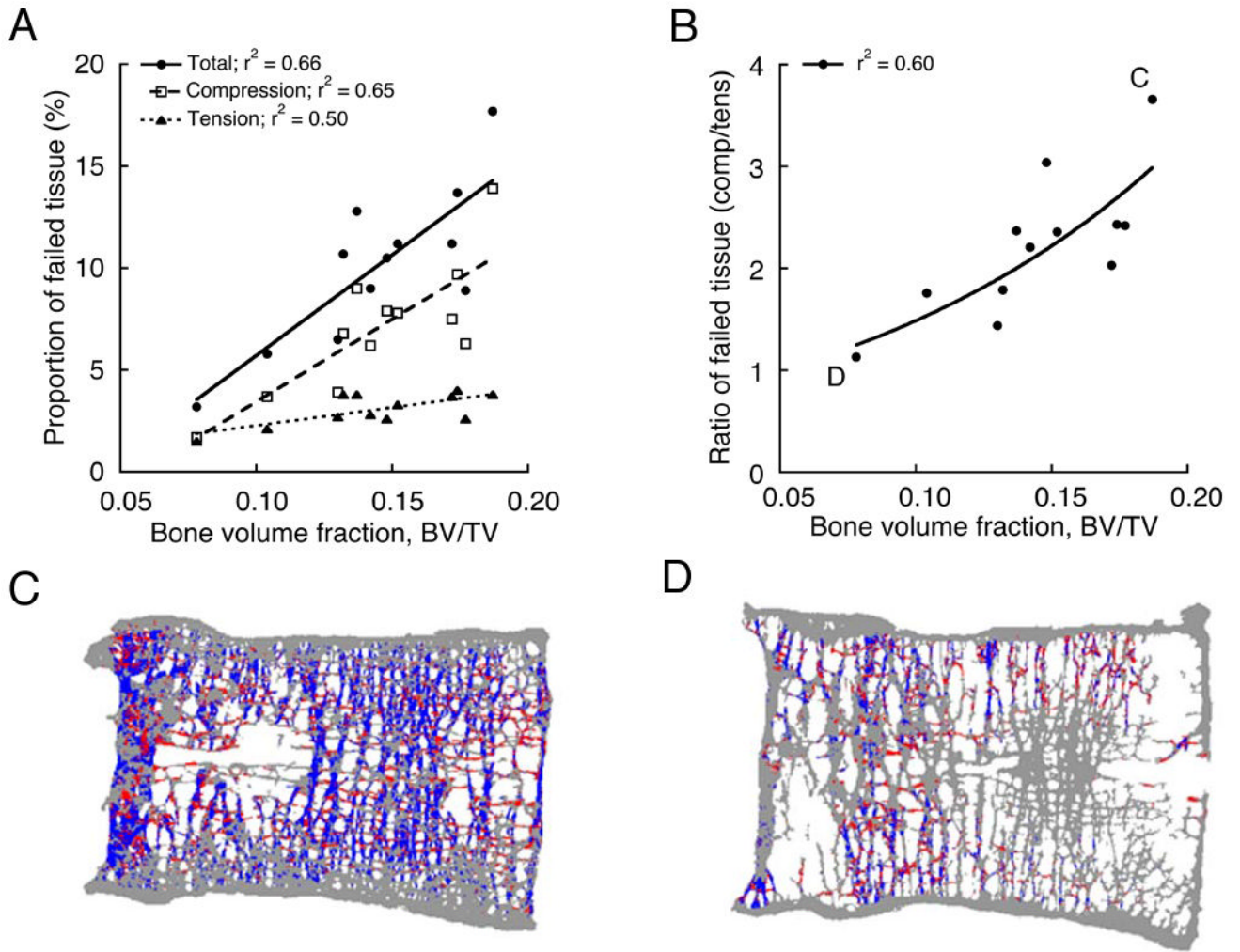


Figure 2.

The variation amongst individuals in the total proportion of failed tissue and in the proportions of failed tissue in compression (blue) and in tension (red). (A) The lower amount of failed tissue in vertebrae with low bone volume fraction primarily reflected less compressive failure. (B) The decrease in the ratio of failed tissue in compression-to-tension revealed a shift in failure mechanisms from axial deformation to bending. (C) Vertebrae with high bone volume fraction yielded via diffuse, compressive deformation of the vertical trabeculae and the cortical shell. (D) Vertebrae with low bone volume fraction yielded via localized bending of the vertical trabeculae. The lines in (A)-(B) represent the best-fit relationships ($p < 0.01$).